

Supporting Information

Compressive-Strain-Engineered TiO₂/rGO Heterojunction

Polysulfide Mediator

Zhengbiao Luo,^a Haoyun Dou,^a Qingye Zhao,^{b,*} Chen Qing,^a Hongqing Ma,^{c,*} and

Hong-En Wang^{a,*}

^a College of Physics and Electronic Information, Yunnan Key Laboratory of Optoelectronic Information Technology, Yunnan Normal University, Kunming 650500, China. Email: hongenwang@whut.edu.cn, hongen.wang@outlook.com

^b Hubei Key Laboratory for Clean Recycling and Resource Utilization of Waste Fibers, College of Chemistry and Chemical Engineering, Wuhan Textile University, Wuhan 430200, China. Email: 2591073007@wtu.edu.cn

^c School of Energy & Environmental Science, Yunnan Normal University, Kunming 650500, China. Email: hongqing6010@126.com

Experimental Section

2.1 Materials

Titanium butoxide ($\text{Ti}(\text{OC}_4\text{H}_9)_4$, TBOT), graphene oxide, glycerol ($\text{C}_3\text{H}_8\text{O}_3$), and potassium hydroxide (KOH) were purchased from Aladdin. All chemicals were of analytical-grade purity and used as received.

2.2 Materials characterizations

The surface morphology of the samples was observed using a scanning electron microscope (SEM, Hitachi S-4800). Transmission electron microscopy (TEM) and high-resolution TEM (HRTEM) micrographs were obtained using a JEM-2100F transmission electron microscope operating at an accelerating voltage of 200 kV. The X-ray diffractograms of the samples were recorded on a Bruker diffractometer using $\text{Cu K}\alpha$ radiation at 40 kV and 40 mA. The sample surface's elemental composition and electronic states were analyzed by X-ray photoelectron spectroscopy (XPS, ThermoFisher Scientific, alpha) using a 15 kV monochromatic $\text{Al K}\alpha$ radiation source. The position of the XPS peak was calibrated against the C 1s peak of the ribbon at 284.8 eV. Raman spectra of the samples were obtained using an INVIA (RENISHAW Corp.) laser Raman spectrometer with an excitation wavelength of 532 nm.

2.3 Synthesis of TNGO and TGO

TNGO was synthesized through a combined hydrothermal and annealing process. Briefly, graphene oxide (rGO) was dispersed in anhydrous ethanol under ultrasonication. Glycerol was then added to the mixture under stirring, followed by tetrabutyl titanate. After further stirring, the solution was transferred to a Teflon-lined autoclave and reacted at 180 °C for 24 h. The obtained product was collected, washed, and dried, then annealed in air at 350 °C for 4 h (heating rate: 1 °C·min⁻¹) to obtain the final TNGO powder.

The TiO₂/rGO composite (termed TGO) was prepared via a physical mixing method. P-TiO₂ was synthesized by hydrothermal treatment of tetrabutyl titanate at 180°C followed by calcination at 450 °C. Thermally reduced graphene oxide (rGO, derived from GO under argon atmosphere at 500 °C) and P-TiO₂ were mixed at a mass ratio of 1:1, and the resulting composite was named TGO.

2.4 Fabrication of TNGO/PP Modified Separator

The TNGO/PP modified separator was fabricated via doctor-blade coating on a commercial polypropylene (PP) membrane. In a typical process, TNGO, Super P, and polyvinylidene fluoride (PVDF) were thoroughly mixed in predetermined mass ratios and ground into a homogeneous powder. An appropriate amount of N-methyl-2-pyrrolidone (NMP) was then added to form a uniform slurry. The slurry was coated onto the PP separator using a doctor blade with a controlled gap thickness,

followed by vacuum drying at 50 °C overnight. The dried membrane was cut into circular discs and further dried under vacuum before being transferred into an argon-filled glove box for cell assembly. For comparison, a rGO/PP separator was prepared under the same conditions using commercial rGO.

2.5 Fabrication of C/S Cathodes

The C/S composite cathodes were fabricated by doctor-blade coating. Carbon-coated aluminum foil was first cut and fixed onto a glass plate, then dried for later use. The active material (C/S composite), Super P, and PVDF were mixed in a mass ratio of 8:1:1. After thorough homogenization, an appropriate amount of N-methyl-2-pyrrolidone (NMP) was added to form a uniform slurry. The slurry was coated onto the prepared foil using a doctor blade with controlled thickness. The coated electrodes were dried overnight at 55 °C, cut into 12 mm diameter discs, and further dried under vacuum at 60 °C for 1 h before being transferred to an argon-filled glove box for cell assembly.

2.6 Assembly of Symmetric Cells

The cells were assembled according to the following procedure: First, the electrode materials TiO₂ and polyvinylidene fluoride (PVDF) were mixed in a 4:1 mass ratio and homogenized in an agate mortar. An appropriate amount of N-methyl-2-pyrrolidone (NMP) was added to form a uniform slurry with suitable viscosity. The slurry was coated onto carbon-coated aluminum foil using a four-sided doctor blade

applicator to ensure even deposition. The coated electrodes were dried overnight at 55 °C in air and cut into 12 mm diameter disks. Subsequently, the electrodes were further dried in a vacuum oven at 55 °C for 1 h and transferred into an argon-filled glovebox for cell assembly.

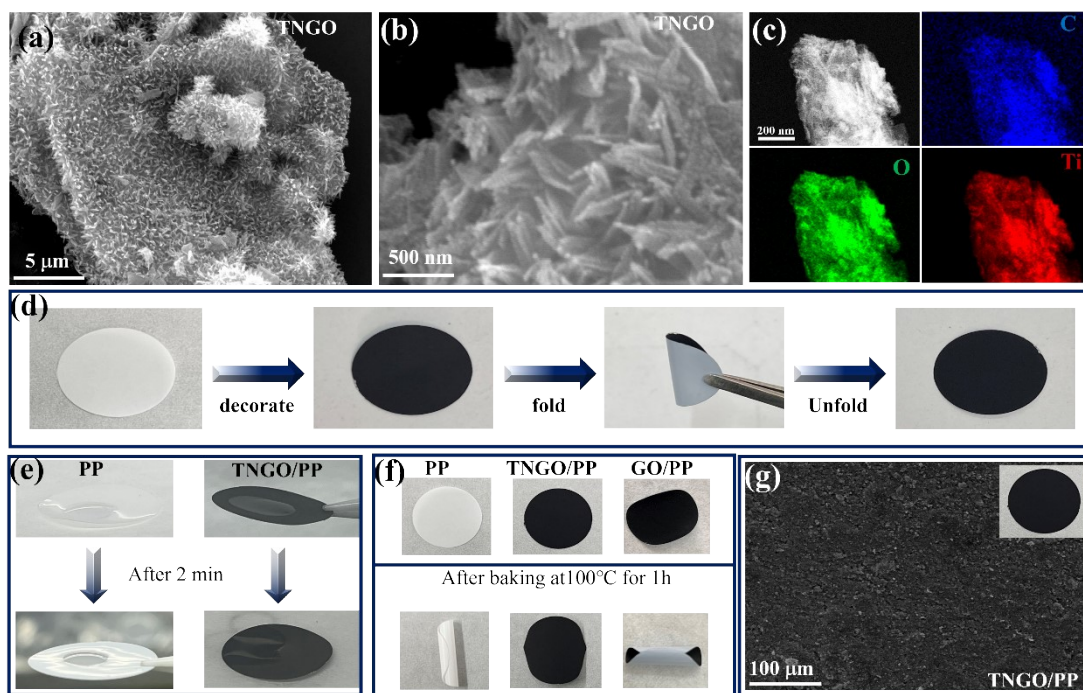


Fig. S1. (a) and (b) SEM images of TNGO; (c) Elemental mapping of TNGO, verifying the uniform distribution of C, O and Ti elements; (d) Folding test of the TNGO/PP separator; (e) Electrolyte wettability test of TNGO/PP separator (performed in a glove box filled with argon gas); (f) Thermal tolerance test of TNGO/PP, GO/PP, and PP separators; (g) SEM image of TNGO/PP separator.

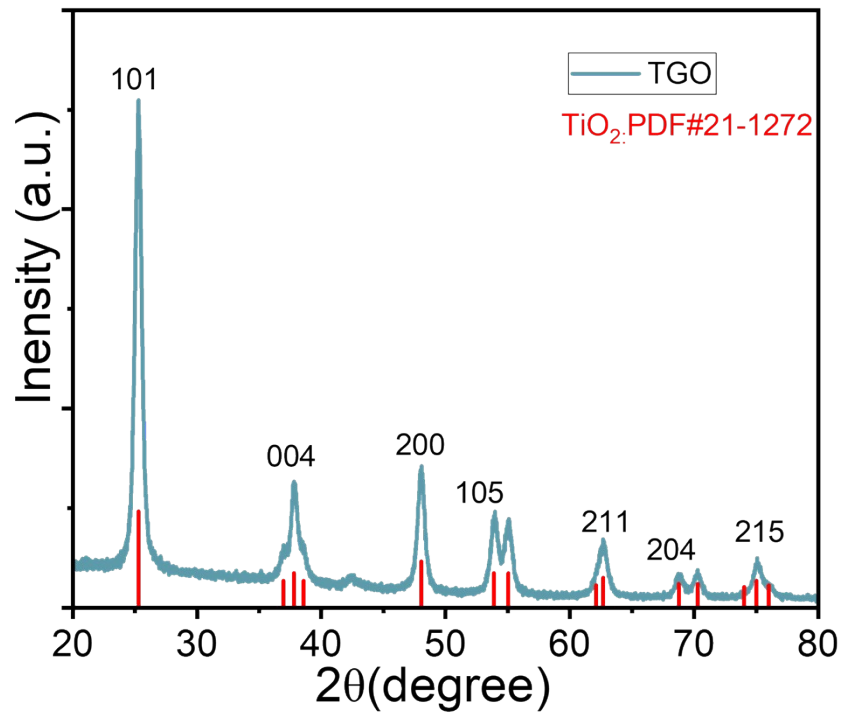


Fig. S2. XRD pattern of the TGO composite, confirming the absence of lattice strain in the TiO₂ phase.

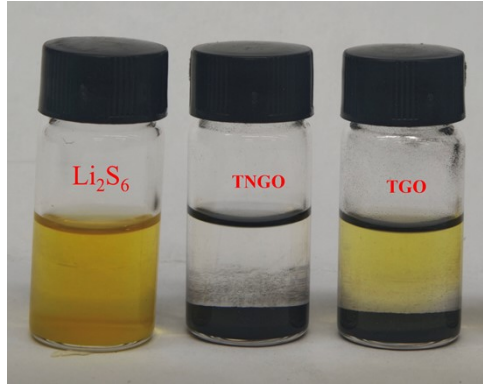


Fig. S3. Digital photograph of Li_2S_6 solution after static adsorption test of TNGO and TGO.

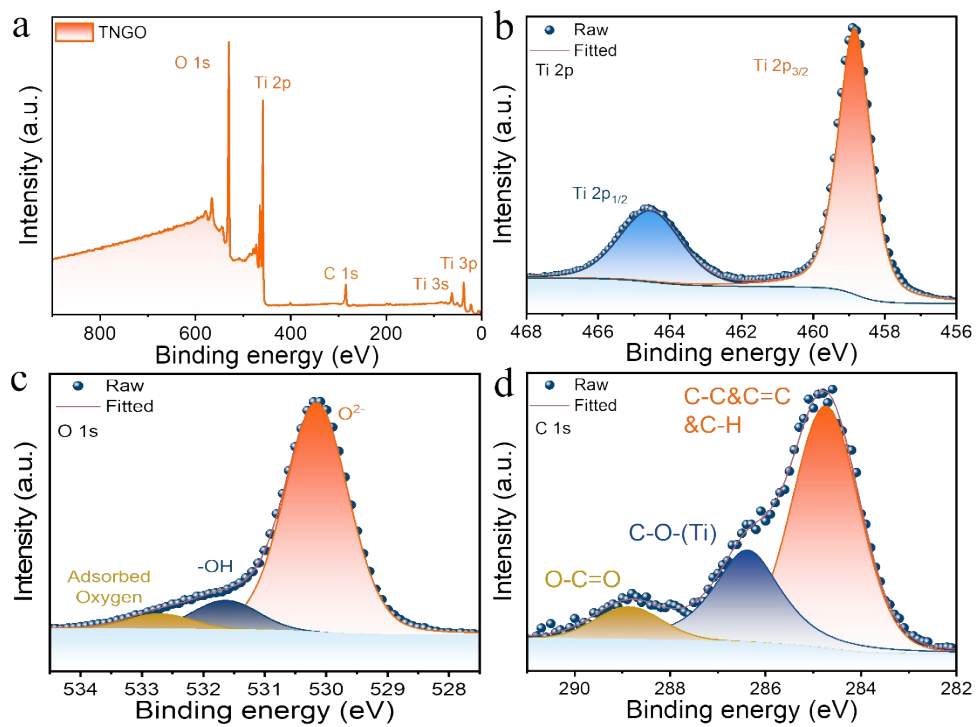


Fig. S4. (a) Survey XPS spectrum of the TNGO sample; high-resolution XPS spectra of (b) Ti 2p, (c) O 1s, and (d) C 1s core levels.

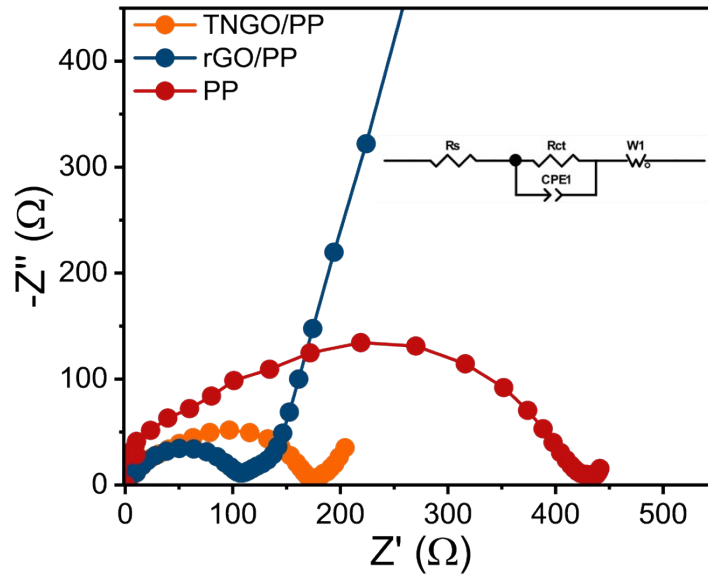


Fig. S5. Electrochemical impedance spectroscopy (EIS) plots of TNGO/PP, rGO/PP, and PP.

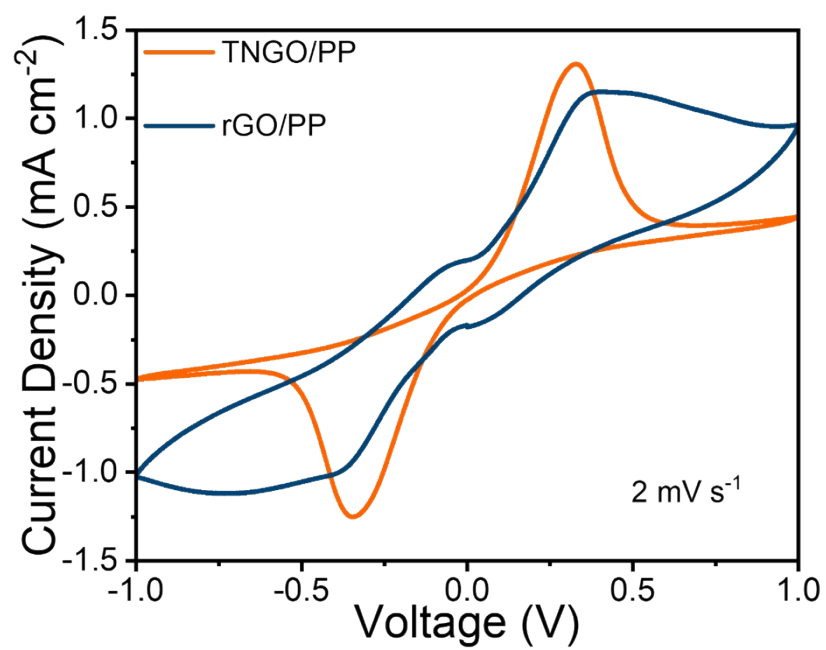


Fig. S6. CV curves of symmetric Li-S cells with TNGO/PP and rGO/PP, respectively.

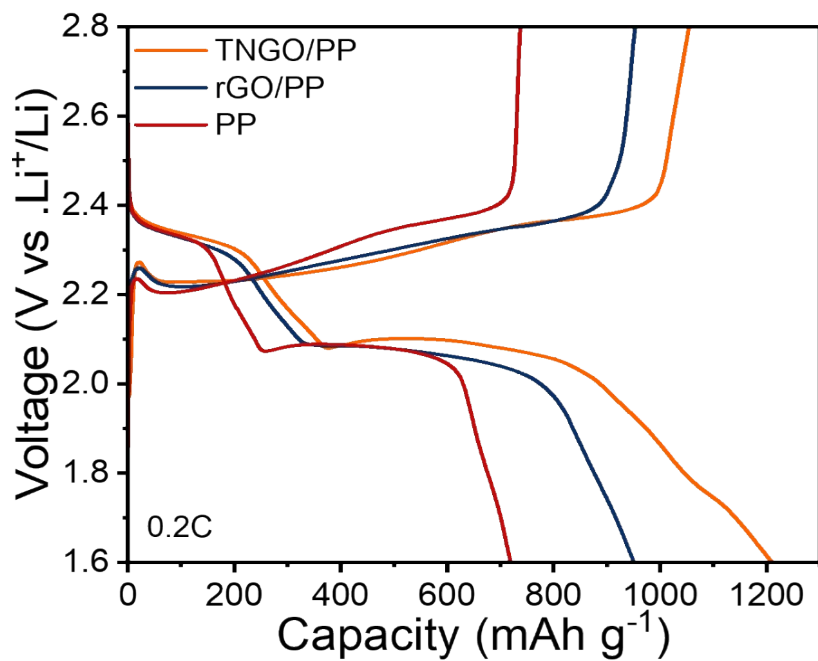


Fig. S7. Galvanostatic charge-discharge profiles of LSBs with TNGO/PP, rGO/PP, and PP separators, respectively.

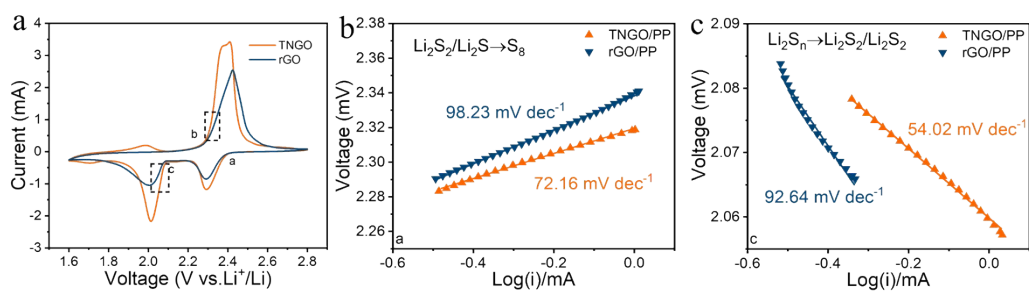


Fig. S8. (a) CV curves at 0.2 mV s⁻¹. (b) The Tafel plots obtained from the high-potential region correspond to the reduction of elemental sulfur to long-chain lithium polysulfides ($S_8 \rightarrow Li_2S_{4-8}$); (c) The Tafel plots obtained from the low-potential region correspond to the reduction of long-chain lithium polysulfides to insoluble Li_2S_2/Li_2S .

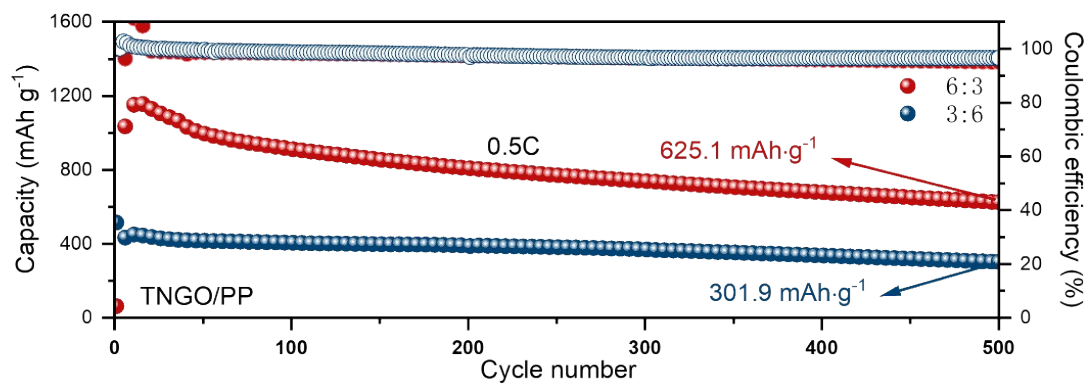


Fig. S9. Performance data for cells with different TNGO: Super P ratios.

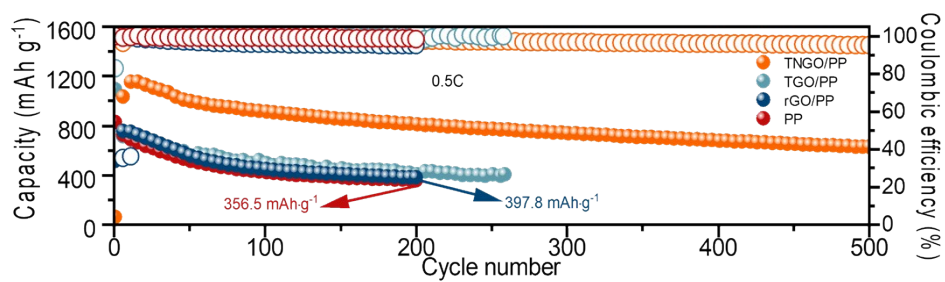


Fig. S10. Long-cycle performance of cells with TNGO/PP, TGO/PP, rGO/PP, and pristine PP separators tested at 0.5 C.

Table S1. Comparison of the electrochemical results in this work with existing literature at 0.5 C and different S mass loadings.

Material	S loading (mg cm ⁻²)	High S loading (C rate) Cycle	Capacity (mAh g ⁻¹)	Ref.
TNGO	4.32	(0.1 C) 200	614.9	This work
Zn@LSC	4.16	(0.1 C) 150	667	1
CoSe ₂ WSe ₂ /NC	4.7	(0.2 C) 150	359.9	2
SnSe ₂ @MXene	5	(0.2 C) 120	751	3
CoRu@N-CNTs	3.072	(1 C) 400	514.5	4
Co-Mo ₂ C@NCNTs	3.2	(0.5 C) 100	655.52	5
Fe-ZIF-8	2.5	(0.1 C) 100	555	6
MnO ₂ @HDGF	NA	NA	660.51	7
3SN1Ti	1.161	(0.5 C) 400	544.3	8
CFP@CN-PP	2.5	(1 C) 400	734	9
Nb ₂ O ₅ /CNT	1.6	(0.5 C) 300	604	10

NA: not available

Table S2. The explicit data of electrolyte-to-sulfur (E/S) ratio, the evolution trend of Coulombic efficiency, and the comparison of electrochemical results with those reported in the existing literature in this work.

Material	E/S ratio ($\mu\text{L mg}^{-1}$)	Capacity decay (per cycle / cycles)	Cycle performance ($\text{mAh g}^{-1}/$ C)	Ref.
TNGO	8.2	0.062%/1000	1072/1.0	This work
uFGF-MoS ₂ /C- TiN	10	0.05%/1000	1000/1.0	11
VGCF/MoS ₂	10	0.03%/600	1208.7/0.2	12
CFM-3M	7	0.066%/200	1259/0.1	13
In ₂ S ₃ /Bi ₂ S ₃ @rGO	7	NA	1205/1.0	14
Co- Mo ₂ C@NCNTs	NA	0.11%/500	1463.6/0.1c	5
Mo ₃ P/Mo	NA	0.414%/100	1357/0.5	15
CoN-Mo ₂ N	NA	0.107%/500	1180/1.0	16
CoSe ₂ WSe ₂ /NC	5	0.081%/800	1072.8/1.0	2
T-MoSe ₂	10	0.065%/400	845.9/1.0	17

NA: not available

References

1. J. Shen, X. Fang, Z. Tang, J. Ou, W. Li, F. Wang and C. Li, *Journal of Power Sources*, 2025, **649**, 237479.
2. R. Wang, H. Xu, Y. Huang, W. Lei, Y. Zou and Y. Wang, *Sustainable Materials and Technologies*, 2025, **46**, e01765.
3. A. Mirtaleb, M. Scekcic and R. Wang, *ENERGY & ENVIRONMENTAL MATERIALS*, 2025, **n/a**, e70173.
4. P. Xia, S. Li, L. Yuan, S. Jing, X. Peng, S. Lu, Y. Zhang and H. Fan, *Journal of Membrane Science*, 2024, **694**, 122395.
5. S. Dong, X. Jin, P. Xia, X. Liu, S. Lu, Y. Zhang and H. Fan, *Journal of Energy Storage*, 2024, **101**, 114000.
6. R. Razaq, M. M. U. Din, D. R. Småbråten, V. Eyupoglu, S. Janakiram, T. O. Sunde, N. Allahgoli, D. Rettenwander and L. Deng, *Advanced Energy Materials*, 2024, **14**, 2302897.
7. R. Li, J. Li, X. Wang, C. Jian, X. Wu, B. Zhong and Y. Chen, *Journal of Colloid and Interface Science*, 2024, **654**, 13-24.
8. P. Zhou, D. Yao, H. Liang, Y. Xia and Y.-P. Zeng, *Ceramics International*, 2023, **49**, 1381-1389.
9. T. Yoo, J. Y. Maeng, S. Park, M. Bae, Y. Kim, J. Choi, H. Hong, S. J. Hwang, E. Lee and Y. Piao, *Journal of Alloys and Compounds*, 2023, **949**, 169873.
10. L. Zhan, X. Zhou, J. Luo, X. Fan and X. Ning, *International Journal of Hydrogen Energy*, 2022, **47**, 27671-27679.
11. M. Waqas, Y. Han, D. Chen, S. Ali, C. Zhen, C. Feng, B. Yuan, J. Han and W. He, *Energy Storage Materials*, 2020, **27**, 333-341.
12. R. Wang, J. Li, Y. Zhang, P. Li, J. Duan, M. Tang and C. Yuan, *Ceramics International*, 2020, **46**, 19408-19415.
13. Y.-C. Ge, R.-X. Wang, X.-C. Huang, J. Zhu, B. He, X.-J. Chen, P.-C. Liu and Y. Meng, *Angewandte Chemie International Edition*, 2026, **65**, e15665.
14. M. A. Al-Tahan, B. Miao, S. Xu, Y. Cao, M. Hou, M. R. Shatat, M. Asad, Y. Luo, A. E. Shrsr and J. Zhang, *Journal of Colloid and Interface Science*, 2024, **654**, 753-763.
15. Z. Sun, Y. Wang, J. Xu and X. Wang, *Frontiers in Chemistry*, 2024, **Volume 12 - 2024**.
16. C. Xu, X. Jiang, M. Huang, W. Luo, S. Zhang, S. Zhao, G. Li and J. Lian, *Chemical Engineering Journal*, 2024, **488**, 151132.
17. R. Li, Z. Bai, W. Hou, Z. Wu, P. Feng, Y. Bai, K. Sun and Z. Wang, *Chinese Chemical Letters*, 2023, **34**, 108263.